Autophagy 8:6, 963–969; June 2012; © 2012 Landes Bioscience

Analysis of macroautophagy by immunohistochemistry

Mathias T. Rosenfeldt, Colin Nixon, Emma Liu, Li Yen Mah and Kevin M. Ryan*
Beatson Institute for Cancer Research; Garscube Estate; Glasgow, UK

(Macro)Autophagy is a phylogenetically conserved membrane-trafficking process that functions to deliver cytoplasmic cargoes to lysosomes for digestion. The process is a major mechanism for turnover of cellular constituents and is therefore critical for maintaining cellular homeostasis. Macroautophagy is characteristically distinct from other forms of autophagy due to the formation of double-membraned vesicles termed autophagosomes which encapsulate cargoes prior to fusion with lysosomes. Autophagosomes contain an integral membrane-bound form (LC3-II) of the microtubule-associated protein 1 light chain 3 β (MAP1LC3B), which has become a gold-standard marker to detect accumulation of autophagosomes and thereby changes in macroautophagy. Due to the role played by macroautophagy in various diseases, the detection of autophagosomes in tissue sections is frequently desired. To date, however, the detection of endogenous LC3-II on paraffin-embedded tissue sections has proved problematic. We report here a simple, optimized and validated method for the detection of LC3-II by immunohistochemistry in human and mouse tissue samples that we believe will be a useful resource for those wishing to study macroautophagy ex vivo.

Keywords: autophagy, LC3, tissue sections, immunohistochemistry

Abbreviations: LC3, microtubule-associated protein 1 light chain 3B; LC3-I, free cytosolic, nonconjugated form of LC3; LC3-II, LC3 conjugated to phosphatidylethanolamine; Atg, autophagy related; EBSS, Earle's balanced salt solution; TbT, Tris-buffered Tween (pH 7.5); MEF, mouse embryonic fibroblast

Submitted: 08/11/11
Revised: 03/27/12
Accepted: 03/28/12
http://dx.doi.org/10.4161/auto.20186

*Correspondence to: Kevin M. Ryan;
Email: k.ryan@beatson.gla.ac.uk

1. Introduction

Autophagy when translated from Greek, literally means 'self-eating' and is a collective term for processes that deliver cellular materials to lysosomes for digestion.[1] To date, three forms of autophagy have been described: macroautophagy, microautophagy and chaperone-mediated autophagy. Each of these processes mediates turnover of cytoplasmic constituents and is therefore critical for maintaining cellular integrity and fidelity.[1] The best-characterized form of autophagy is macroautophagy. Macroautophagy is a morphologically and genetically defined process which is coordinated by a series of autophagy-related (*ATG*) genes, many of which are conserved through evolution.[2,3] Although operating at basal levels in virtually all cells, the levels and effects of macroautophagy can be modulated so that the cell can adapt to specific environments and cues.[4]

Macroautophagy, different from other forms of autophagy, is characterized by the formation of double-membraned vesicles termed autophagosomes.[3] These vesicles serve to carry cargoes destined for digestion at the lysosome.[3] Upon initiation, membranes termed phagophores are formed from various sources within the cell.[5-8] As these membranes grow, a cleaved form of the protein MAP1LC3B (termed LC3-I), which is expressed diffusely in the cytoplasm, is conjugated to the lipid phosphatidylethanolamine.[9,10] The protein is now termed LC3-II, and through its lipid conjugate integrates into the phagophore membrane.[9,10] Once the autophagosome is formed, it can undergo fusion events with other vesicles including endosomes and multivesicular bodies, but ultimately autophagosomes fuse with lysosomes to form autolysosomes.[3] It is in autolysosomes that the cargo of the autophagosome is digested by acid hydrolases provided by the lysosome, and the breakdown products are then transferred back into the cytoplasm where they can either be recycled or further catabolized to fuel metabolism.

The classical method used to detect autophagosomes is electron microscopy.[11,12] However, since electron microscopy is time consuming and costly, its use as the primary method to detect macroautophagy declined upon the development of antibodies which can detect both LC3-I and LC3-II.[9,11,12] These antibodies have been deployed primarily for use in western blotting where LC3-I and LC3-II can be discerned due to different mobility, or in fluorescent microscopy studies where LC3-I appears diffuse in the cytoplasm and LC3-II appears as distinct puncta indicative of formation of autophagosomes.[11,12]

Numerous studies have shown that macroautophagy protects against a spectrum of diseases including neurodegenerative diseases and cancer.[1,13-18] Perturbations in macroautophagy regulators have also been reported in various human malignancies and in the chronic inflammatory bowel disorder Crohn disease.[19-25] As a result, considerable interest has surrounded the role played by macroautophagy in these and other conditions. The ability, however, to detect LC3-labeled autophagosomes in paraffin-embedded tissue has so far proved problematic. The situation instigated the production of a transgenic mouse line that contains a GFP-LC3 transgene that is expressed in all tissues to facilitate detection of macroautophagy.[26] Detection of endogenous LC3-I/LC3-II, however, is still preferable and is the only option for analysis of paraffin-embedded human tissue. Although staining for LC3 by immunohistochemistry has been reported,[27-31] to the best of our knowledge no protocol has so far been published which details a method for immunohistochemistry of LC3 on human and mouse tissue sections. Since there is an increasing demand to analyze autophagy in human biopsies and in transgenic animal models, we were keen to optimize a technique for the detection of endogenous LC3-I/LC3-II in ex vivo material. We present here a detailed protocol for the staining of endogenous LC3, which we show can be used to detect and quantify changes in autophagosome number in paraffin-embedded tissue samples.

2. Materials

2.1. Equipment. (1) Standard microtome. (2) PT Module (Thermo, PT-module) or alternatively a 800 W microwave oven with a microwavable pressure cooker. (3) Excelsior ES tissue processor (Thermo scientific). (4) Histology cassette system (CellPath, EAD/0102/04H). (5) Leica EG1160 wax embedder. (6) Humidified slide chambers (sealed box containing damp paper towels).

2.2. Slides. All slides used were silane coated (CellPath, MDC-0102-54A).

2.3. Antibodies. (1) LC3 mouse monoclonal (Nanotools, 5F10). (2) ATG7 rabbit polyclonal (Santa Cruz Biotechnology, sc-33211). (3) p62 antibody (ENZO BML-PW98600). (4) Ubiquitin antibody (Novus Biologicals, NB300-130). (5) MAPK14/p38 antibody (Cell Signaling, CS9212). (6) Secondary antibodies: EnVision blocking and secondary antibody kit [Dako, K4007 (anti-mouse) or K4011 (anti-rabbit)]. EnVision kit K4001 was used for secondary antibody (anti-mouse) staining of human tissue (Dako, K4001). (7) Primary antibody diluent (Dako, S2022).

2.4 Staining chemicals. (1) 3,3'-Diaminobenzidine tetrahydrochloride (Dako, K3468). (2) Haem Z hematoxylin (CellPath, RBA-4201-00A). (3) DPX mountant for microscopy (BDH, 360294H). (4) Block for endogenous peroxidase (Dako S2023). (5) BLOXALL blocking reagent for endogenous peroxidase (human tissue) (Vector Labs, SP-6000).

2.5. Standard chemicals. (1) 10% Neutral-buffered formalin (neutral-buffered formaldehyde 10% v/v (Surgipath/Leica 00600E). (2) Xylene. (3) Ethanol. (4) Tris-buffered Tween (TbT), pH 7.5 (Dako S3306). (5) 1% acid alcohol (1% concentrated HCl in 70% ethanol). (6) Scott's tap water substitute (166 mM $MgSO_4$ (Sigma, 208094), 45 mM $NaHCO_3$ in deionized water). (7) 10 mM Na Citrate buffer (pH 6). (8) 10 mM Tris-EDTA, pH 9 (or in some instances pH 6). (9) Deionized water. (10) Paraffin embedding wax was from Leica, 08605E.

2.6. Cells and tissue samples. Wild-type and *atg7*$^{-/-}$ MEFs were harvested from E13.5 *ATG7*$^{fl/fl}$ transgenic mice (kindly provided by Masaaki Komatsu, Tokyo Metropolitan Institute of Medical Science). These cells and HeLa cells (which can be obtained from ATCC) were maintained in Dulbecco's-modified Eagle Medium supplemented with 10% fetal calf serum at 37°C in an atmosphere of 5% CO_2 in air. Where indicated, cells were incubated in EBSS to induce autophagy. The human liver sample used in this staining was archived prior to the Human Tissue (Scotland) Act 2006 and so its use within this manuscript fits within our institutional and Scottish government guidelines.

3. Methods

3.1. Sample preparation. *3.1.1.* Fixation of tissues/organs. Tissues/organs should be placed in small pieces (approximately 3 mm^3) immediately into 10% neutral buffered formalin and fixed for 24–48 h at room temperature.

3.1.2. Processing of tissues/organs. Tissues/organs are then put into histology cassettes (Histology Cassette System II, CellPath, EAD/0102/04H) and processed in a Thermo Excelsior ES tissue processor (or processed by hand; see section 5 'Concluding Remarks/Notes') as follows:

(1) 10% neutral buffered formalin for 30 min.
(2) 70% ethanol for 35 min.
(3) 90% ethanol for 40 min.
(4) 95% ethanol for 45 min.
(5) 100% ethanol for 50 min.
(6) 100% ethanol for 50 min.
(7) 100% ethanol for 55 min.
(8) Xylene for 45 min.
(9) Xylene for 50 min.
(10) Xylene for 60 min.
(11) Wax for 1 h, 15 min.
(12) Wax for 1 h, 25 min.
(13) Wax for 1 h, 40 min.
(14) Samples are then taken out of the Excelsior ES (the wax is molten at that stage).

3.1.3. Embedding/orientation of tissues/organs. (1) Samples are taken out of the histology cassettes and put into a small metal tray (the size of a histology cassette) containing molten wax and reoriented in order to obtain the correct direction of the samples on the slides. Histology cassettes

are then placed around the samples again and more wax is added using a Leica EG1160 wax embedder. (All this is done while the wax is molten.) (2) The wax is then left to harden at −5°C for at least 5 min. The sample can, however, be left to harden for up to 2 h.

3.2. Antibody staining. *3.2.1.* Cutting sections. 4-μm sections are cut on a standard microtome and placed at 60°C in a dry oven for a minimum of 1 h.

3.2.2. Staining of sections. (1) Place sections in xylene for 5 min being careful to cover the entire section. (2) Place sections in 100% ethanol for 1 min. (3) Place sections again in 100% ethanol for 1 min. (4) Place sections in 70% ethanol for 1 min. (5) Wash sections in running tap water for 5 min. (6) Heat-induced epitope retrieval: place section in PT module for 25 min at 98°C. Alternatively, for detecting LC3, sections can be placed in 10 mM Tris-EDTA, pH 9 and for detecting ATG7 in 10 mM Na Citrate buffer (pH 6), for 4 min after full pressure has been attained in a microwavable pressure chamber. (7) In PT module leave the sections to cool to 65°C. Alternatively, for microwave-based retrieval, leave the sections in buffer to cool for 20 min. (8) Wash sections in 10 mM TbT, pH7.5 for 5 min. (9) Block for endogenous peroxidase (Dako, S2023) for 5 min. For human tissue incubate in BLOXALL blocking solution for 5 min. (10) Wash sections in TbT 5 min. (11) Apply LC3 antibody (1:100 in primary antibody diluent) for 45 min at room temperature. For ATG7, dilute antibody 1:75 in primary antibody diluent and incubate for 45 min at room temperature. **NOTE:** It is critically important in all staining procedures that an additional slide is stained in the absence of a primary antibody to control for false-positive staining being produced from the secondary antibody. (12) Wash sections twice in TbT for 5 min. (13) Apply secondary antibody (Dako EnVision) for 30 min. (14) Wash sections twice in TbT for 5 min. (15) Apply 3,3'-diaminobenzidine tetrahydrochloride for 10 min. (16) Terminate reaction with deionized water, 1 min. (17) Place sections in haem Z hematoxylin for 5 min. (18) Wash sections in deionized water for 1 min. (19) Place sections in 1% acid alcohol, 3 dips. (20) Wash sections in deionized water for 1 min. (21) Place sections in Scott's tap water substitute for 2 min. (22) Wash sections in deionized water for at least 30 sec. (23) Dehydrate sections in 70% ethanol for 3–5 min, twice in 100% ethanol for 3–5 min, clean in xylene for 3–5 min and mount.

4. Results

In order to optimize a technique for immunohistochemical staining of endogenous LC3, we utilized wild-type and *atg7*$^{-/-}$ mouse embryonic fibroblasts (MEFs) which can be respectively considered macroautophagy-competent and macroautophagy-deficient due to the critical role of ATG7 in the conversion of LC3-I to LC3-II and which, as a result, exhibit differences in the ability to degrade the autophagic cargo SQSTM1/p62 (**Fig. 1A**).[32] These cells were maintained in either regular replete medium or Earle's balanced salt solution (EBSS) as an autophagic stimulus and were then embedded in paraffin wax and processed as would be the case for ex vivo material. This gave us a system in which to optimize staining of paraffin-embedded sections with wild-type cells in EBSS acting as a positive control for autophagosome accumulation and *atg7*$^{-/-}$ cells acting as a negative control. After several approaches in which we tried various antibodies, incubation times, blocking reagents, epitope extraction methods and chromogen stains, conditions were resolved where autophagosomes were clearly identifiable and distinguishable from nonspecific staining artifacts (**Fig. 1B**). Using the materials and methods as outlined in the following sections, the conditions we had optimized for LC3-staining in paraffin-embedded cells were applied to archived, paraffin-embedded mouse tissue. The mouse tissue analyzed was derived from animals that contain two *Atg7* floxed alleles and a whole-body, inducible Cre recombinase. In this system, Cre is fused to a portion of the human estrogen receptor (ER) such that its activity can be induced by the estrogen analog, 4-hydroxytamoxifen.[33] Since the Cre-ER fusion is driven from a CAGG promoter, which is expressed throughout the body, the *Atg7* locus can be recombined in all tissues of adult mice upon treatment with 4-hydroxytamoxifen. In many tissues, however, the Cre-ER is expressed at varying levels and it is unlikely that 4-hydroxytamoxifen administration reaches all cells. As a result, a mosaic pattern is observed in which some regions

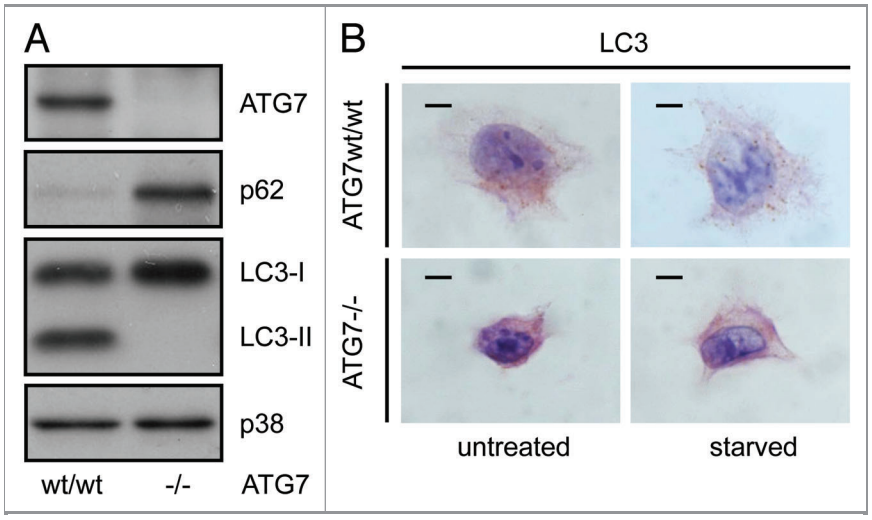

Figure 1. LC3 immunohistochemical staining shows a punctate pattern in wild-type MEFs and a homogenous staining pattern in *atg7*$^{-/-}$ MEFs. (A) Western blot of ATG7, SQSTM1/p62, LC3-I and LC3-II and MAPK14/p38 in wild-type and *atg7*$^{-/-}$ MEFs. (B) Representative images of immunohistochemical detection of LC3 in wild-type and *atg7*$^{-/-}$ MEFs that were cultured in replete medium (untreated) or starved in EBSS for 2 h. Antigen retrieval was undertaken in Tris-EDTA, pH 9. Images were taken at 100x magnification and the scale bars in each panel represent 20 μm.

of tissue have lost *Atg7* through recombination and other regions are unaffected and retain a floxed (wild-type) allele (**Fig. 2**, regions positive for ATG7 are marked with a red dotted line and are labeled with asterisks). Staining of sequential sections of pancreatic tissue for LC3 from mice that had been treated with 4-hydroxytamoxifen for 2 weeks revealed that puncta indicative of autophagosomes could clearly be detected in tissue competent for macroautophagy (marked with a red dotted line and are labeled with asterisks), whereas this was not the case for tissue devoid of the essential autophagy gene *Atg7* (**Fig. 2**). In these regions, LC3-I staining was homogeneous reflecting its diffuse distribution in the cytoplasm (**Fig. 2**). In addition, large LC3-positive aggregates could also be detected in *atg7*$^{-/-}$ tissue (**Fig. 2**, bottom row, 2nd panel from the left), similar to what has been reported in tissue lacking Atg5 and in situations where LC3 associates with protein aggregates containing SQSTM1.[34,35] No LC3-positive staining was observed in either wild-type or *atg7*$^{-/-}$ tissue in the absence of primary antibody indicating that the staining was not a nonspecific stain from the secondary antibody (**Fig. S1**).

In further sequential sections from the same tissue block, regions of pancreas lacking ATG7 also displayed accumulation of SQSTM1 and ubiquitinated aggregates, underscoring the fact that these regions which also lack LC3-positive puncta and show diffuse, homogenous LC3 staining, are autophagy-deficient (**Fig. 2**). We also applied the protocol to paraffin-embedded liver, which had been derived from the same mice. This once again revealed that small LC3-positive puncta were evident in regions containing ATG7 (although less than that observed in pancreatic tissue), whereas stronger, homogeneous, cytoplasmic LC3 staining was observed in tissue lacking ATG7 (**Fig. 3**). Since the number of LC3-positive puncta was quite small in wild-type tissue (particularly in the case of liver), we wanted to further confirm the specificity and sensitivity of our protocol by analyzing tissue from wild-type mice that had been starved for 14 h to cause induction of autophagy. In both pancreas and liver from starved mice, we observed a significantly enhanced accumulation of LC3-positive puncta when compared with tissues from mice that had access to food ad libitum (**Fig. 4**). We were also able to quantify the difference in puncta between these two feeding states, which revealed, as would be expected, a statistically

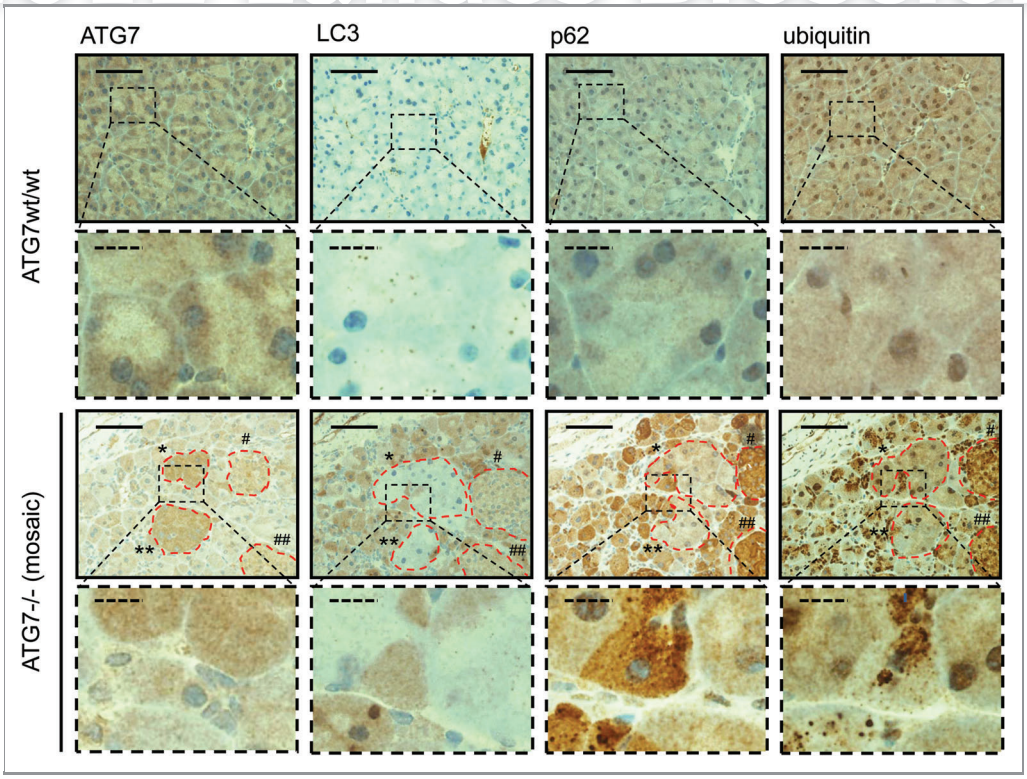

Figure 2. Detection of a punctate LC3-staining pattern in murine wild-type pancreas and uniform staining in *atg7*$^{-/-}$ tissue. Immunohistochemical staining for ATG7, LC3, SQSTM1/p62 and ubiquitin in murine wild-type pancreata (top two rows) and in consecutive sections from pancreata with mosaic deletion of *ATG7* (*atg7*$^{-/-}$, bottom two rows). Panels with straight borders are complete, i. e. not cropped and representative overview images taken at 40x magnification with a scale bar (straight) that represents 100 μm. Panels with dashed borders are zoomed and cropped sections from the overview panels (cropped regions are indicated by the small dashed rectangle in the overview panels). The dashed scale bars in the cropped panels represent 20 μm. IHC was done on consecutive sections for the *atg7*$^{-/-}$ samples and each display two large, not recombined (i.e., *Atg7*$^{wt/wt}$) regions of pancreatic acinar tissue that are marked as (*, **) and encircled in red. In addition two pancreatic islets (#, ##) are also marked and encircled which act as landmark structures to enable clear alignment of sequential sections. Antigen retrieval for LC3 was undertaken in Tris-EDTA, pH 9 for LC3 and in 10 mM Na Citrate buffer, pH 6 for ATG7, SQSTM1/p62 and ubiquitin.

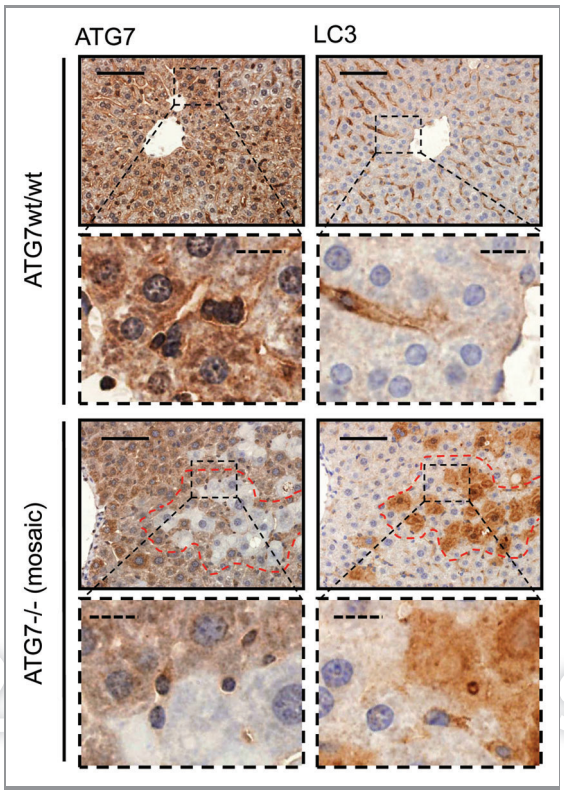

Figure 3. Detection of a punctate LC3-staining pattern in murine wild-type liver and uniform staining in *atg7*$^{-/-}$ tissue. Immunohistochemical staining for ATG7 and LC3 in murine wild-type liver (top two rows) and consecutive liver sections with mosaic deletion of *ATG7* (*atg7*$^{-/-}$, bottom two rows). Panels with straight borders are complete, i.e., not cropped and representative overview images taken at 40x magnification with a scale bar (straight) that represents 100 μm. Panels with dashed borders are cropped sections from the overview panels (cropped regions are indicated by the small dashed rectangle). The dashed scale bars in the zoomed and cropped panels represent 20 μm. IHC was done on consecutive sections for the *atg7*$^{-/-}$ samples and a landmark region with mostly recombined (i.e. ATG7-deficient) cells is encircled with red dashes. Antigen retrieval for LC3 was undertaken in Tris-EDTA, pH 9 and at 10 mM Na Citrate buffer, pH 6 for ATG7.

significant increase in puncta ($p < 0.05$) in starved mice compared with control (**Fig. 4**). When taken together these observations clearly indicate that this protocol is a reliable method to detect different levels of LC3-puncta and therefore autophagosomes in tissue samples from mice.

We have also applied this protocol to human cells and tissue with positive results. HeLa cervival carcinoma cells were incubated in either replete medium or EBSS for 2 h to induce autophagy and were then embedded in paraffin wax. Sections from these paraffin blocks were processed and stained for LC3 and this revealed a marked and statistically significant increase ($p < 0.01$) in LC3-positive puncta in EBSS-treated cells representing the accumulation of autophagosomes associated with induction of autophagy (**Fig. 5A**). Archived sections of normal human liver were also stained using this protocol and clear LC3-positive puncta were observed which were not seen in the absence of primary antibody, indicating that the protocol can be utilized for the detection of autophagosomes in both human and mouse paraffin-embedded tissue (**Fig. 5B**).

5. Concluding Remarks/Notes

We acknowledge that the specific equipment used in perfecting this technique may not be available to all investigators. In particular, the tissue processing steps can in fact be performed by hand. If processing by hand or if different equipment is employed, then some refinement of the technique may be required, particularly if analysis involves tissues other than those described in this report. We think, however, that optimum antigen retrieval is the critical step in obtaining successful results. In this regard, we consider that other heat retrieval methods may be used and may even be more successful in certain situations. However, if antigen retrieval is achieved with water baths or automated retrieval modules then we consider that retrieval temperatures should be set at 98°C. In addition to this antigen/epitope retrieval step, we would also recommend that all tissues are fixed in 10% formalin for a minimum of 24 h prior to staining. For consistent results, we also suggest carrying out the complete staining protocol in one session that does not involve 'stop-starts.' Moreover, if direct comparisons are required between sections, we strongly suggest that these are stained at the same time and to reiterate, we also cannot overemphasize the need for a control lacking primary antibody in each staining run, in order to have the ability to detect false-positives in each assay. Lastly, we would also like to state that it is not the intention of our protocol to specifically endorse the antibody we use above other LC3 antibodies that are currently available. In fact, LC3 staining in specific contexts has been reported with other antibodies.[27-31] We would advise caution, however, that if other antibodies are used with the protocol we describe here, additional conditions and optimization steps may then be required.

As a final cautionary note, we would like to mention the limitations of LC3 staining in general. While staining for LC3 is currently the only assay available for analyzing autophagy in paraffin-embedded tissue, the appearance of LC3-positive puncta does not necessarily indicate that the tissue contain high levels of active, successful autophagy. Autophagosomes (as represented by LC3-positive puncta) constitute a mid-point in the autophagy process and as such, can accumulate due to induction of autophagy or, because most cells have a basal autophagy rate, due to inhibition of autophagy at a point downstream of autophagosome accumulation. This can occur, for example, due to impairment of fusion

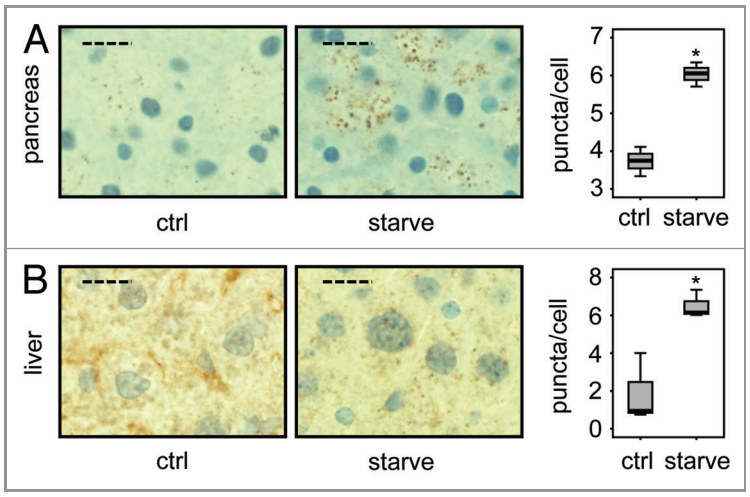

Figure 4. LC3 staining reveals quantitative differences in endogenous LC3 puncta formation. Representative immunohistochemical staining for LC3 in murine pancreas (A) and liver (B) from control mice (i.e., with access to food ad libitum) and mice starved for 14 h (but with free access to water). The panels are representative crops from images taken at 40x magnification and the dashed scale bars represent 20 μm. Box plots are used to display the quantification of LC3-puncta/cell for each condition. "*" indicates statistical significance ($p < 0.05$, Mann-Whitney). LC3-positive puncta of at least 150 cells (exocrine pancreas or hepatocytes respectively) from each of three mice in every group were counted. Antigen retrieval for LC3 was undertaken in Tris-EDTA, pH 9.

between autophagosomes and lysosomes or compromised lysosomal activity in general. It is the complete digestion of autophagic cargoes that constitutes the autophagy process and so-called 'autophagic flux' through this pathway that is the critical factor in understanding whether autophagy is active or not in any given situation. In this regard, we refer the reader to the consortium article by Klionsky et al., which discusses the pros and cons of LC3-staining and other autophagy assays.[11] While bearing in mind these limitations, in the current absence of an assay for autophagic flux in paraffin-embedded tissue, we nonetheless believe that the protocol we present here constitutes a useful step forward in the ability to analyze autophagy in both normal and diseased tissue from human and mouse.

Supplemental Materials

Supplemental materials may be found here: www.landesbioscience.com/journals/autophagy/article/20186

Acknowledgments

Work in the Tumour Cell Death Laboratory is supported by Cancer Research UK and the Association for International Cancer Research. We are grateful to Owen Sansom for help with our mouse studies and to Masaaki Komatsu for kindly providing *Atg7*$^{flox/flox}$ mice that were used to generate MEFs and tissue stained in this study. We are also thankful to Saira Ghafoor and Ambreen Siddiq for help with immunostaining and we would like to dedicate this study to the memory of Ambreen who sadly, unexpectedly passed away while the manuscript was under revision.

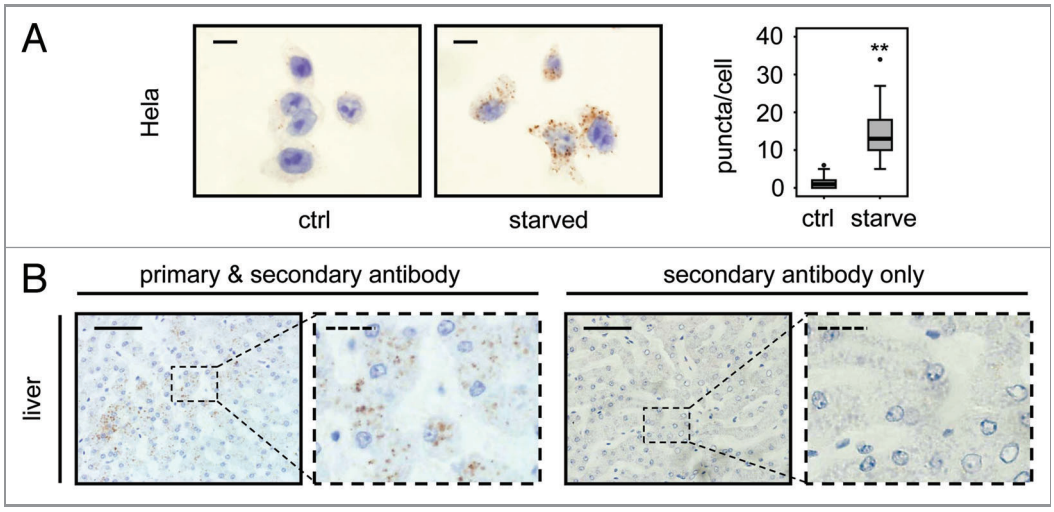

Figure 5. LC3 staining allows quantification of endogenous LC3 puncta in human cells and detects LC3 positive puncta in human tissue. (A) Representative immunohistochemical staining for LC3 in HeLa cells that were grown in replete medium or starved for 2 h in EBSS. Images were taken at 100x magnification and the scale bars represent 20 μm. Box plots are used to display the quantification of LC3-puncta/cell for each condition. "**" indicates statistical significance ($p < 0.01$, Mann-Whitney). LC3-positive puncta of 50 cells from each group were counted. (B) Human liver stained with LC3 antibody (left two panels) and without primary antibody as control (right two panels). Panels with straight borders are complete, i.e., not cropped and representative overview images taken at 40x magnification with a scale bar (straight) that represents 100 μm. Panels with dashed borders are zoomed and cropped sections from the overview panels (cropped regions are indicated by the small dashed rectangle in the overview panels). The dashed scale bars in the cropped panels represent 20 μm. Antigen retrieval for LC3 was undertaken in Tris-EDTA, pH 9.

References

1. Mizushima N, Levine B, Cuervo AM, Klionsky DJ. Autophagy fights disease through cellular self-digestion. Nature 2008; 451:1069-75; PMID:18305538; http://dx.doi.org/10.1038/nature06639
2. Yang Z, Klionsky DJ. Eaten alive: a history of macroautophagy. Nat Cell Biol 2010; 12:814-22; PMID:20811353; http://dx.doi.org/10.1038/ncb0910-814
3. Xie Z, Klionsky DJ. Autophagosome formation: core machinery and adaptations. Nat Cell Biol 2007; 9:1102-9; PMID:17909521; http://dx.doi.org/10.1038/ncb1007-1102
4. Yang Z, Klionsky DJ. Mammalian autophagy: core molecular machinery and signaling regulation. Curr Opin Cell Biol 2010; 22:124-31; PMID:20034776; http://dx.doi.org/10.1016/j.ceb.2009.11.014
5. Axe EL, Walker SA, Manifava M, Chandra P, Roderick HL, Habermann A, et al. Autophagosome formation from membrane compartments enriched in phosphatidylinositol 3-phosphate and dynamically connected to the endoplasmic reticulum. J Cell Biol 2008; 182:685-701; PMID:18725538; http://dx.doi.org/10.1083/jcb.200803137
6. Hailey DW, Rambold AS, Satpute-Krishnan P, Mitra K, Sougrat R, Kim PK, et al. Mitochondria supply membranes for autophagosome biogenesis during starvation. Cell 2010; 141:656-67; PMID:20478256; http://dx.doi.org/10.1016/j.cell.2010.04.009
7. Tooze SA, Yoshimori T. The origin of the autophagosomal membrane. Nat Cell Biol 2010; 12:831-5; PMID:20811355; http://dx.doi.org/10.1038/ncb0910-831
8. Ravikumar B, Moreau K, Jahreiss L, Puri C, Rubinsztein DC. Plasma membrane contributes to the formation of pre-autophagosomal structures. Nat Cell Biol 2010; 12:747-57; PMID:20639872; http://dx.doi.org/10.1038/ncb2078
9. Kabeya Y, Mizushima N, Ueno T, Yamamoto A, Kirisako T, Noda T, et al. LC3, a mammalian homologue of yeast Apg8p, is localized in autophagosome membranes after processing. EMBO J 2000; 19:5720-8; PMID:11060023; http://dx.doi.org/10.1093/emboj/19.21.5720
10. Kabeya Y, Mizushima N, Yamamoto A, Oshitani-Okamoto S, Ohsumi Y, Yoshimori T. LC3, GABARAP and GATE16 localize to autophagosomal membrane depending on form-II formation. J Cell Sci 2004; 117:2805-12; PMID:15169837; http://dx.doi.org/10.1242/jcs.01131
11. Klionsky DJ, Abdalla H, Abeliovich H, Abraham RT, Acevedo-Arozena A, Adeli K, et al. Guidelines for the use and interpretation of assays for monitoring autophagy. Autophagy 2012; 8; In press; PMID: 18188003
12. Mizushima N, Yoshimori T, Levine B. Methods in mammalian autophagy research. Cell 2010; 140:313-26; PMID:20144757; http://dx.doi.org/10.1016/j.cell.2010.01.028
13. Levine B, Kroemer G. Autophagy in the pathogenesis of disease. Cell 2008; 132:27-42; PMID:18191218; http://dx.doi.org/10.1016/j.cell.2007.12.018
14. Cadwell K, Stappenbeck TS, Virgin HW. Role of autophagy and autophagy genes in inflammatory bowel disease. Curr Top Microbiol Immunol 2009; 335:141-67; PMID:19802564; http://dx.doi.org/10.1007/978-3-642-00302-8_7
15. Mathew R, Karantza-Wadsworth V, White E. Role of autophagy in cancer. Nat Rev Cancer 2007; 7:961-7; PMID:17972889; http://dx.doi.org/10.1038/nrc2254
16. Ravikumar B, Sarkar S, Davies JE, Futter M, Garcia-Arencibia M, Green-Thompson ZW, et al. Regulation of mammalian autophagy in physiology and pathophysiology. Physiol Rev 2010; 90:1383-435; PMID: 20959619; http://dx.doi.org/10.1152/physrev.00030.2009
17. Rosenfeldt MT, Ryan KM. The role of autophagy in tumour development and cancer therapy. Expert Rev Mol Med 2009; 11:e36; PMID:19951459; http://dx.doi.org/10.1017/S1462399409001306
18. Wong E, Cuervo AM. Autophagy gone awry in neurodegenerative diseases. Nat Neurosci 2010; 13:805-11; PMID:20581817; http://dx.doi.org/10.1038/nn.2575
19. Kang MR, Kim MS, Oh JE, Kim YR, Song SY, Kim SS, et al. Frameshift mutations of autophagy-related genes ATG2B, ATG5, ATG9B and ATG12 in gastric and colorectal cancers with microsatellite instability. J Pathol 2009; 217:702-6; PMID:19197948; http://dx.doi.org/10.1002/path.2509
20. Aita VM, Liang XH, Murty VV, Pincus DL, Yu W, Cayanis E, et al. Cloning and genomic organization of beclin 1, a candidate tumor suppressor gene on chromosome 17q21. Genomics 1999; 59:59-65; PMID:10395800; http://dx.doi.org/10.1006/geno.1999.5851
21. Liang XH, Jackson S, Seaman M, Brown K, Kempkes B, Hibshoosh H, et al. Induction of autophagy and inhibition of tumorigenesis by beclin 1. Nature 1999; 402:672-6; PMID:10604474; http://dx.doi.org/10.1038/45257
22. Crighton D, Wilkinson S, Ryan KM. DRAM links autophagy to p53 and programmed cell death. Autophagy 2007; 3:72-4; PMID:17102582
23. Cadwell K, Liu JY, Brown SL, Miyoshi H, Loh J, Lennerz JK, et al. A key role for autophagy and the autophagy gene Atg16l1 in mouse and human intestinal Paneth cells. Nature 2008; 456:259-63; PMID: 18849966; http://dx.doi.org/10.1038/nature07416
24. Barrett JC, Hansoul S, Nicolae DL, Cho JH, Duerr RH, Rioux JD, et al, NIDDK IBD Genetics Consortium, Belgian-French IBD Consortium, Wellcome Trust Case Control Consortium. Genome-wide association defines more than 30 distinct susceptibility loci for Crohn's disease. Nat Genet 2008; 40:955-62; PMID:18587394; http://dx.doi.org/10.1038/ng.175
25. Kim MS, Jeong EG, Ahn CH, Kim SS, Lee SH, Yoo NJ. Frameshift mutation of UVRAG, an autophagy-related gene, in gastric carcinomas with microsatellite instability. Hum Pathol 2008; 39:1059-63; PMID: 18495205; http://dx.doi.org/10.1016/j.humpath.2007.11.013
26. Mizushima N, Yamamoto A, Matsui M, Yoshimori T, Ohsumi Y. In vivo analysis of autophagy in response to nutrient starvation using transgenic mice expressing a fluorescent autophagosome marker. Mol Biol Cell 2004; 15:1101-11; PMID:14699058; http://dx.doi.org/10.1091/mbc.E03-09-0704
27. Holt SV, Wyspianska B, Randall KJ, James D, Foster JR, Wilkinson RW. The development of an immunohistochemical method to detect the autophagy-associated protein LC3-II in human tumor xenografts. Toxicol Pathol 2011; 39:516-23; PMID:21441228; http://dx.doi.org/10.1177/0192623310396903
28. Nahdi A, Hammami I, Kouidhi W, Chargui A, Ben Ammar A, Hamdaoui MH, et al. Protective effects of crude garlic by reducing iron-mediated oxidative stress, proliferation and autophagy in rats. J Mol Histol 2010; 41:233-45; PMID:20700633; http://dx.doi.org/10.1007/s10735-010-9283-5
29. Chargui A, Zekri S, Jacquillet G, Rubera I, Ilie M, Belaid A, et al. Cadmium-induced autophagy in rat kidney: an early biomarker of subtoxic exposure. Toxicol Sci 2011; 121:31-42; PMID:21325019; http://dx.doi.org/10.1093/toxsci/kfr031
30. Kim JH, Kim JH, Yu YS, Mun JY, Kim KW. Autophagy-induced regression of hyaloid vessels in early ocular development. Autophagy 2010; 6:922-8; PMID:20818164; http://dx.doi.org/10.4161/auto.6.7.13306
31. Mookerjee S, Papanikolaou T, Guyenet SJ, Sampath V, Lin A, Vitelli C, et al. Posttranslational modification of ataxin-7 at lysine 257 prevents autophagy-mediated turnover of an N-terminal caspase-7 cleavage fragment. J Neurosci 2009; 29:15134-44; PMID:19955365; http://dx.doi.org/10.1523/JNEUROSCI.4720-09.2009
32. Komatsu M, Waguri S, Ueno T, Iwata J, Murata S, Tanida I, et al. Impairment of starvation-induced and constitutive autophagy in Atg7-deficient mice. J Cell Biol 2005; 169:425-34; PMID:15866887; http://dx.doi.org/10.1083/jcb.200412022
33. Hayashi S, McMahon AP. Efficient recombination in diverse tissues by a tamoxifen-inducible form of Cre: a tool for temporally regulated gene activation/inactivation in the mouse. Dev Biol 2002; 244:305-18; PMID: 11944939; http://dx.doi.org/10.1006/dbio.2002.0597
34. Kuma A, Matsui M, Mizushima N. LC3, an autophagosome marker, can be incorporated into protein aggregates independent of autophagy: caution in the interpretation of LC3 localization. Autophagy 2007; 3:323-8; PMID:17387262
35. Shvets E, Elazar Z. Autophagy-independent incorporation of GFP-LC3 into protein aggregates is dependent on its interaction with p62/SQSTM1. Autophagy 2008; 4:1054-6; PMID:18776740